

Water FlowInduced Energy Harvesting Exploiting Stacked Graphene Oxide Membranes

*Original*

Water FlowInduced Energy Harvesting Exploiting Stacked Graphene Oxide Membranes / Lezzoche, Antonio; Aixala Perello, Anna; Pedico, Alessandro; Laurenti, Marco; Raffone, Federico; Lamberti, Andrea. - In: ADVANCED SUSTAINABLE SYSTEMS. - ISSN 2366-7486. - (2023), pp. 1-8. [10.1002/adsu.202300046]

*Availability:*

This version is available at: 11583/2978496 since: 2023-05-22T10:50:59Z

*Publisher:*

Wiley

*Published*

DOI:10.1002/adsu.202300046

*Terms of use:*

openAccess

This article is made available under terms and conditions as specified in the corresponding bibliographic description in the repository

*Publisher copyright*

(Article begins on next page)

# Water Flow-Induced Energy Harvesting Exploiting Stacked Graphene Oxide Membranes

Antonio Lezzoche, Anna Aixalà-Perelló, Alessandro Pedico, Marco Laurenti, Federico Raffone, and Andrea Lamberti\*

Energy harvesting from water flow or evaporation is recently reported exploiting carbon-based materials. The water-carbon dualism is at the base of this phenomenon thanks to a charge redistribution at the liquid/solid interface. Many kinds of approaches and nanomaterials are proposed for this purpose. The main properties under investigation are the surface functionalization and the porosity of carbon-based materials. In this context, the exploitation of a stacked graphene oxide (GO) membrane as layered nanochannels for water flow energy harvesting is proposed. At the best of this study's knowledge, GO membranes are never reported for this application. The flow is spontaneously induced by both capillarity and evaporation when part of the membrane is incubated in water. In this study, zero-energy is externally provided allowing sustainable energy production without sub-products. Different GO membranes are tested for this purpose reaching a maximum open circuit voltage of  $\approx 450$  mV and maximum current of  $\approx 100$  nA.

forward. In the last decades, there has been a growing interest in the so-called "Blue Energy", which is linked to all the natural phenomena related to water that releases energy.<sup>[2-4]</sup> Most of the research in this sector is focused on the energy harvesting from sea waves, sea tides, temperature gradient, and salinity gradient. The last one, in particular, is emerging thanks to its huge potential.<sup>[5]</sup> It consists in recovering energy by mixing two different solutions: freshwater and salty water. From a theoretical point of view, from the interaction between river (freshwater) and sea (saltwater) up to  $0.8 \text{ kW m}^3$  could be extracted.<sup>[3]</sup> The principle behind this phenomenon is the entropy increase of the system with equal enthalpy that leads to a free energy decrease. This energy is known as Gibbs free energy of

## 1. Introduction

Nowadays, energy issues and environmental problems are two of the most crucial points to deal with. In 2018, <15% of the sources of the total energy supply were renewable. Being so addicted to coal, oil, and natural gas led to an emission of 33 513 Mt of  $\text{CO}_2$  in that year.<sup>[1]</sup> For these reasons, a drastic change and a new strategy are needed forcing us to harvest energy from renewable sources. Due to the fact that 71% of the Earth is water-covered, recovering the potential energy stored in the water is a suggested way


mixing, and it is the one that can be captured. To do that, three are the foremost technologies: Pressure Retarded Osmosis (PRO), Reverse Electrodialysis (RED), and Capacitive Mixing (CapMix). Even if huge efforts have been spent to improve these technologies, only RED and PRO have reached the requested level for the installation of the first pilot plants, with many remaining problems related to the membranes used in such systems.<sup>[6]</sup>

For these reasons, more recently a new branch of research was developed exploiting water flow and/or evaporation in carbon-based materials, avoiding the kinetic or chemical energy needed in the previously cited approaches.<sup>[7-9]</sup> It is possible to distinguish three different types of water motion resulting useful for energy harvesting purpose: the droplets movement, the water flow, and the phase change.<sup>[2]</sup> They are strictly related to the so-called streaming potential, this is, the potential arising from charge redistribution at the liquid-solid interface in nanochannels. Furthermore, thanks to the evolution of materials synthesis, it has been observed that carbon-based nanomaterials can play a fundamental role in this specific area because of their multiple properties.

Devices based on the water-carbon dualism are the foundation of many applications that merge into Blue Energy. The idea was to exploit the streaming potential, a particular phenomenon in which there is an electrical potential due to the transition by a pressure gradient of a solution through narrow pores or gaps.<sup>[10]</sup> In their work, Liu et al. observed a small voltage in the range of mV by moving a droplet of a NaCl solution along a graphene monolayer.<sup>[2]</sup> The droplet was enclosed between a graphene

A. Lezzoche, A. Aixalà-Perelló, A. Pedico, M. Laurenti, F. Raffone, A. Lamberti  
Politecnico di Torino  
Dipartimento di Scienza Applicata e Tecnologia (DISAT)  
Corso Duca Degli Abruzzi 24, Torino 10129, Italy  
E-mail: andrea.lamberti@polito.it

A. Aixalà-Perelló, M. Laurenti, F. Raffone, A. Lamberti  
Istituto Italiano di Tecnologia  
Center for Sustainable Future Technologies  
Via Livorno 60, Torino 10140, Italy

 The ORCID identification number(s) for the author(s) of this article can be found under <https://doi.org/10.1002/adsu.202300046>

© 2023 The Authors. Advanced Sustainable Systems published by Wiley-VCH GmbH. This is an open access article under the terms of the Creative Commons Attribution License, which permits use, distribution and reproduction in any medium, provided the original work is properly cited.

DOI: 10.1002/adsu.202300046

surface and a SiO<sub>2</sub>/Si wafer and was moved both from left to right and in the opposite direction, showing the same induced voltage in magnitude. The key parameters for these potential generations are the number of droplets and the velocity. The more droplets are involved in this kind of device, the higher the recorded voltage up to a critical value, and then the voltage decreases as the number of droplets further increases, and at the same time, it increases linearly with the moving velocity.

Another phenomenon, observed by Xue and coworkers in a different setup, is related to water evaporation from different nanostructured carbon materials.<sup>[11]</sup> They showed that it is possible to generate a constant voltage (without any other external power source) taking advantage of the interaction of water molecules and carbon layers. The authors stated that, by a suitable selection of some properties of a carbon material in contact with water and well-designed experimental conditions, it is possible to observe a continuous power generation. Electricity generation is strictly related to streaming current and potential. When the water is forced to pass through micro or nano-pores, charge redistribution at the interface occurs leading to a power generation.<sup>[12]</sup> Although other possible mechanisms were proposed in literature, such as coulombic scattering<sup>[13]</sup> and electron drag by phonon wind,<sup>[14]</sup> and although there is still debate on which one is dominating when water flows continuously in a channel, streaming potential has already been recognized as the source of electricity generation in water evaporation setups.<sup>[9,15]</sup>

Herein, we investigate the application of stacked graphene oxide (GO) layer to harvest energy from the interaction between water molecules and GO layers exploiting the evaporation-induced water flow within the bi-dimensional channels.

GO, the oxidized form of graphene, has been largely investigated for environmental and electrochemical applications.<sup>[16,17]</sup> In fact, it offers different advantages such as high dispersibility, facile synthesis, good mechanical strength, and many oxygen functional groups on its reactive surface.

GO consists of a matrix of oxygen containing functional groups on the basal planes and the edges.<sup>[18]</sup> Typically, the functional groups found at the basal plane are hydroxy and epoxy, while carboxy and carbonyl groups are at the sheet edges.<sup>[19]</sup> Spontaneous GO functional groups give it a hydrophilic nature that enables the interaction of the material with water molecules. Moreover, these functionalities permit the stacking of GO flakes through hydrogen bonding in the sp<sup>3</sup> regions and π–π stacking in the sp<sup>2</sup> clusters allowing the formation of nanochannels in the range of nanometers.

Vacuum filtration of GO dispersion allows the formation of a stacked arrangements of the flakes resulting in membranes that have been deeply studied for separation purpose. Nevertheless, for this study, Dr. Blade casting has been suggested as a scalable alternative technique.<sup>[20]</sup>

Reduced graphene oxide (rGO) sponges have been developed to generate electricity via natural water evaporation.<sup>[9]</sup> In their study, they show the effect of ambient temperatures, airflow velocities, and evaporation-areas on the energy generation, reaching an open-circuit potential of 0.63 V and a maximum output power and output power density of 17.30 μW and 1.74 μW cm<sup>-2</sup>. Instead, Qi et al.<sup>[7]</sup> studied the effect of temperature in such systems. They developed a supermolecular assembly of poly (3,4-ethylenedioxythiophene): poly (styrene sulfone) and graphene ox-

ide able to generate 2.13 V under a temperature difference of 110 K. Instead, it has been proposed elsewhere<sup>[8]</sup> the use of filter paper matrix with naturally deposited reduced graphene oxide that achieved a maximum current density and maximum power density of 325 mA cm<sup>-2</sup> and 53 mW cm<sup>-2</sup>. They exploit the capillary flow on the filter that acts as natural splitter of the flow into tiny droplets.

Herein, we proposed a graphene oxide staked membrane as active material for energy harvesting from water. To the best of our knowledge, graphene oxide (GO) has not yet been studied for water flow-induced energy harvesting up to now. Some of the properties that make GO a promising material for this application are the surface functionalization and the porosity, which corresponds to the interlayer distance among the flakes. For these reasons, GO, either in other allotropes, such as sponges,<sup>[9]</sup> or mixed with other materials, example, PEDOT:PSS/GO,<sup>[7]</sup> has already been applied for electricity generation. However, GO as membrane offers several advantages over the other forms. GO membranes generally show a larger hydrophilicity due to the numerous epoxide and hydroxyl functional groups. Given the layered structure, the water is forced to move in between the sheets in a highly directional passage leading to stronger and more frequent wall-water interactions. We show that thanks to the spontaneous water flow induced by capillarity and evaporation when part of the membrane is incubated in water it is possible to achieve a maximum open circuit voltage of ≈450 mV and maximum current of ≈100 nA. We emphasize that the mechanism of electricity generation in the GO membranes proposed in our work differs significantly from the one occurring with ion-filtering membranes that selectively allow only one of the two ions to pass.<sup>[18]</sup> In the latter case, the nanocapillarity of the membrane is used to sieve the ions based on their effective radius. As a result, at the two ends of the liquid a potential difference arises. In our case, nanocapillarity enhances evaporation so to increase the flux of water leading to a larger downstream charge accumulation.

## 2. Results and Discussion

The fabrication procedure selected for membrane preparation was the doctor blade approach.<sup>[20]</sup> This technique consists of a casting of a gel on a substrate by using a blade at a specific thickness. A blade-to-substrate thickness of 1 mm was set for this study and afterward, the film was dried at room temperature. The majority of the papers reporting GO membrane fabrication exploit vacuum filtration.<sup>[21]</sup> However, that approach cannot be considered scalable and is time- and energy-consuming if thick membranes have to be produced. On the contrary, doctor blade allows a fast fabrication, without the need for pressure difference, and a good control in a wide range of membrane thicknesses. **Figure 1a** shows the GO membrane fabrication method by Dr. Blade technique while in **Figure 1b** the resulting GO membrane is displayed. The membrane was mechanically detached from the glass substrate used for the casting and exhibited very good mechanical properties (see inset of **Figure 1c**). The membrane is constituted by stacked GO flakes as shown in **Figure 1d**.

FTIR spectroscopy (**Figure 2a**) was performed with the purpose of checking the type of functional groups present in our GO membranes. FTIR analysis highlighted the presence of

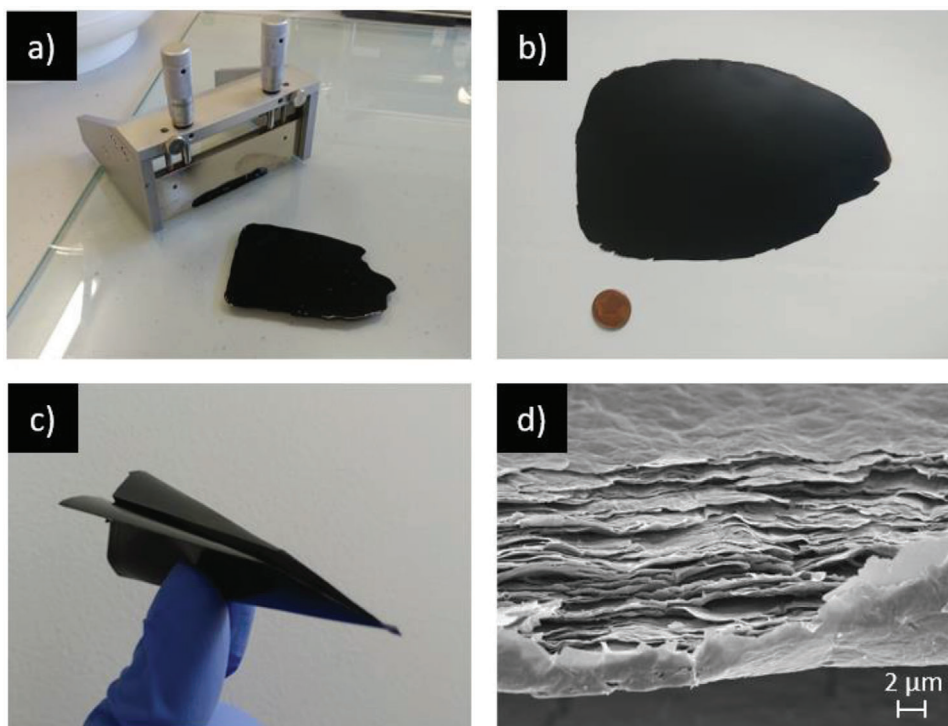


**Figure 1.** GO membranes. a) Membrane fabrication process: the membrane is produced by doctor blade of GO gel on glass substrate. b) Self-standing scalable membrane after drying on a glass substrate. c) Origami figure to show membrane robustness. d) Stacked flakes structure of a cross-section image of the GO membrane by FESEM.

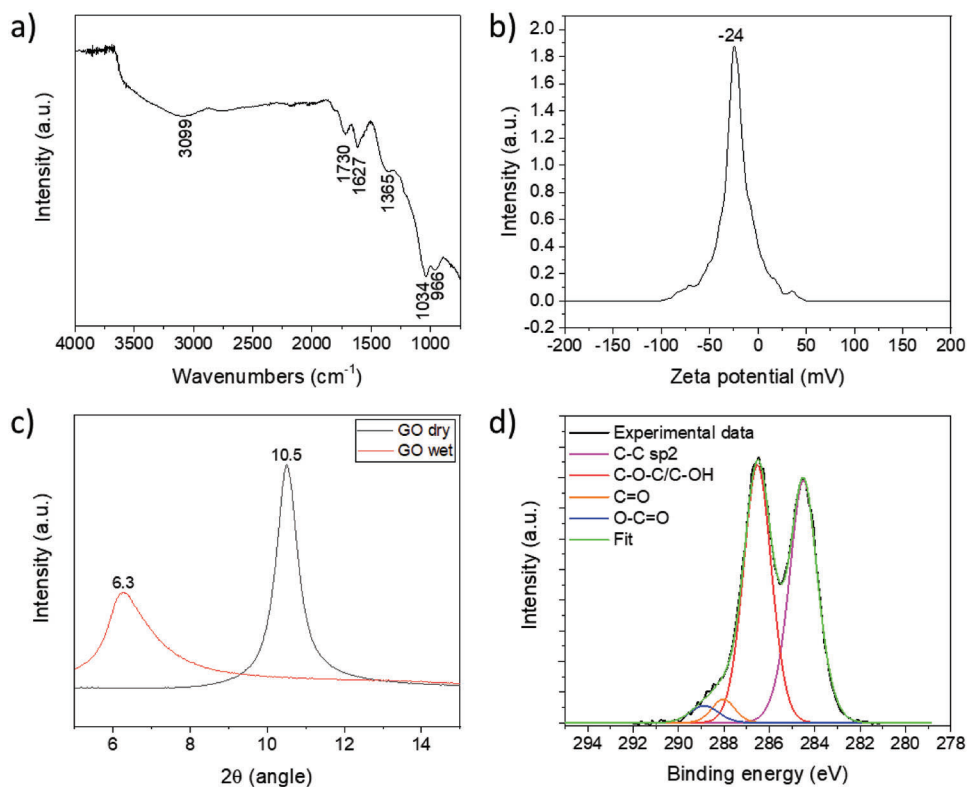


**Figure 2.** Physico-chemical characterization of the GO membranes. a) IR spectra. b) Z-potential. c) XRD. d) XPS spectra.

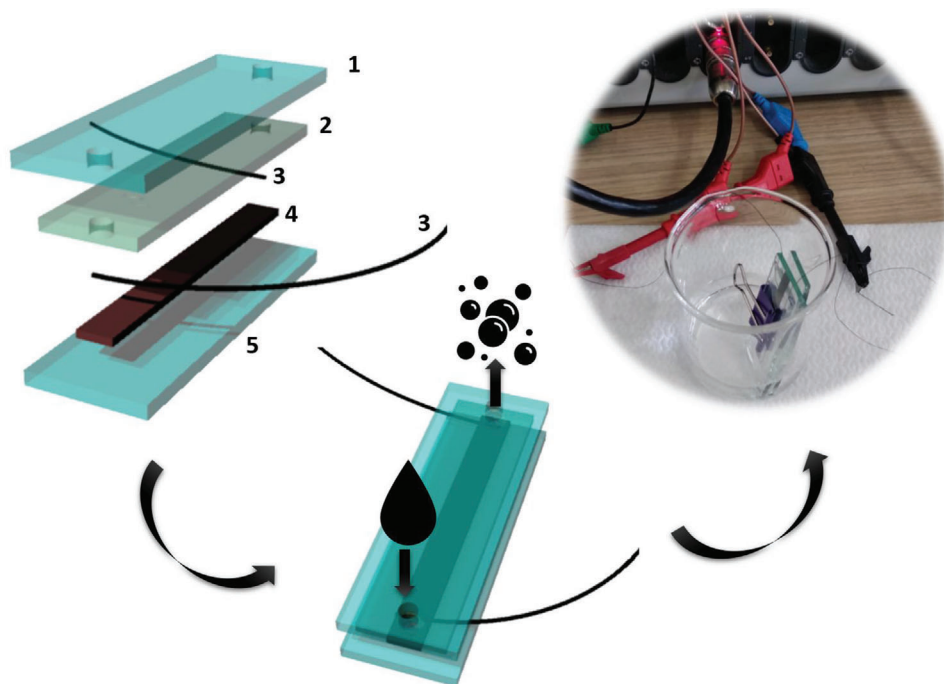


**Figure 3.** 3D rendering of the experimental setup. The stacked structure of the device is composed of a top glass slide with inlet and outlet holes (1), a PDMS slide with aligned holes (2), two CNT yarn current collectors (3), a GO membrane (4), and a bottom glass slide (5). All the elements are aligned and stacked as shown in the figure and then pressed with a clip before incubation in the water solution (see digital photograph).

hydroxyl ( $3500\text{--}2500$  and  $1365\text{ cm}^{-1}$ ), carbonyl ( $1730\text{ cm}^{-1}$ ), alkenyl ( $1627\text{ cm}^{-1}$ ), and epoxy ( $1034$  and  $966\text{ cm}^{-1}$ ) groups.<sup>[22]</sup>

Such groups result in a net surface charge of the GO dispersion with a Z-potential (Figure 2b) equal to  $-24\text{ mV}$ , in accordance with previous literature.<sup>[17]</sup> Such value is responsible for the high stability of GO dispersions in water since the Z-potential evaluates the electrostatic potential near the surface of suspended particles. Consequently, agglomeration in water is prevented by electrostatic repulsion among GO flakes, caused by the presence of negatively charged groups on the flakes' surface.

In order to deeply investigate with quantitative analysis the number of functional groups a thorough analysis was needed. Starting from its chemical composition, the main elements present inside it are Carbon (C), Oxygen (O), and Sulphur (S) (its presence is due to the GO fabrication technique). The C 1s peaks were investigated in order to analyze the functional groups present. The two main peaks were centered at  $284.50$  and  $286.53\text{ eV}$ . They referred to carbon atoms arranged through C–C  $\sigma$  bonds and to epoxy (C–O–C)/hydroxyl (C–OH) groups respectively. The other peaks were atoms involved in C=O ( $288.06\text{ eV}$ ) and carboxyl groups ( $288.50\text{ eV}$ ). The abundant presence of these functional groups was the key to the process of induced-voltage generation described.

Finally, XRD measurement was performed to evaluate the interlayer distance ( $d$ ) of GO. This distance was found to be  $8.4\text{ \AA}$  in the dry membrane and increase up to  $14.0\text{ \AA}$  in the wet state (Figure 2c), with a standard deviation of  $0.1\text{ \AA}$ . Such channel height allows GO membranes to be used for water-flow-induced electricity generation, as described in previous work on porous carbon materials.<sup>[11]</sup>

The water-flow-induced electricity generation was investigated with the experimental setup described in Figure 3. The layout is similar to the one previously proposed for porous carbon layers,<sup>[11]</sup> but with some differences. First of all, the membrane is not directly fabricated on the device substrate but was previously prepared, cut and then transferred as a self-standing membrane on the glass used in the device. Two CNT yarns are used to take the positive and negative contact and a PDMS slice was used as a gasket in order to protect the two carbon wires from water contact and to confine the path of the water only to the GO membrane. These elements are then sandwiched between two rigid supports and clamped to avoid leakages.

Since it is quite simple to modify the thickness without affecting all the other properties of the membrane, we decided to investigate its effect on electricity generation.

Four membranes were fabricated in order to understand if a correlation between the thickness and the open-circuit voltage exists. The working mechanism is expected to be streaming potential as already suggested in literature for other evaporation setups.<sup>[9]</sup> Figure 4 illustrates the suggested mechanism. Water evaporation induces a downstream accumulation of ions that shield the GO charge. This results in a potential difference between the two ends of the membrane that leads to a current in the external circuit. The charge unbalance is maintained as long as the water flows. When the flux ceases, coulombic repulsion forces the ions to evenly distribute on the membrane so that the potential is equal in all the regions and the current stops.<sup>[12]</sup> In Figure 5 it is possible to see an actual trend: higher OCPs are reached for higher thicknesses. These results can be ascribed to the presence of a larger number of graphene flakes in thicker membranes that promote a larger water flow and a higher

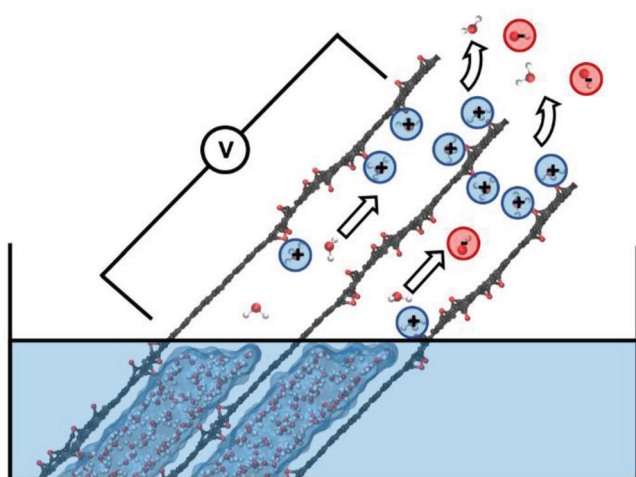


**Figure 4.** Schematic of the suggested mechanism of electricity generation.

number of water/carbon interactions. The 15  $\mu\text{m}$  membrane results to be too brittle and it is easily damaged in water. For this reason, lower dimensions are not recommended. At the same time, pushing to thicker membranes hoping for better voltages is not either good choice. In fact, from 50  $\mu\text{m}$  the membranes present bubbles and structural defects. There is so a trade-off between the mechanical stability of the membrane and the defects due to its fabrication method.

In Figure 5c the current–voltage plot of the 50  $\mu\text{m}$  thick membrane is showed. The open-circuit voltage ( $V_{\text{OC}}$ ) of 0.27 V is almost the same as the one obtained with the OCP measurement (0.23 V), confirming the coherence with the OCP experiment. A value  $\approx 5.49$  nA was found as short-circuit current ( $I_{\text{SC}}$ ). This implies that the device is working correctly: a current generation effectively occurs without other external inputs, leading to a maximum output power of 1.1  $\mu\text{W m}^{-2}$ .

The length of the used glasses for the device fabrication was 7 cm, therefore 6.5 cm was the maximum size usable for the GO membrane in accordance with the device size. All the membranes analyzed in the previous section had a length of 6.5 cm and a width of 0.5 cm.

Afterward, a comparison was made between membranes with the same thickness (50  $\mu\text{m}$ ) and different lengths: 6.5 and 4.5 cm (see Figure S3 in the Supporting Information), showing a slight increase in the OCP and without a substantial difference in the current. This result suggests that the length of the channel does not affect the generation while it is the number of channels (i.e., the thickness of the membrane) that governs the phenomenon.

The next issue investigated involved the substitution of the deionized (DI) water with simulated sea water, this is, a solution of NaCl 0.6 M, in order to investigate its effect on the induced voltage. (Figure 6a). In this case, the interaction between the solution and the GO layers seems to enhance the performance. In the I–V measurement the same  $V_{\text{OC}}$  was found, confirming the validity of the experiment, while a higher  $I_{\text{SC}}$  was registered, a value about two orders of magnitude higher for the same membrane

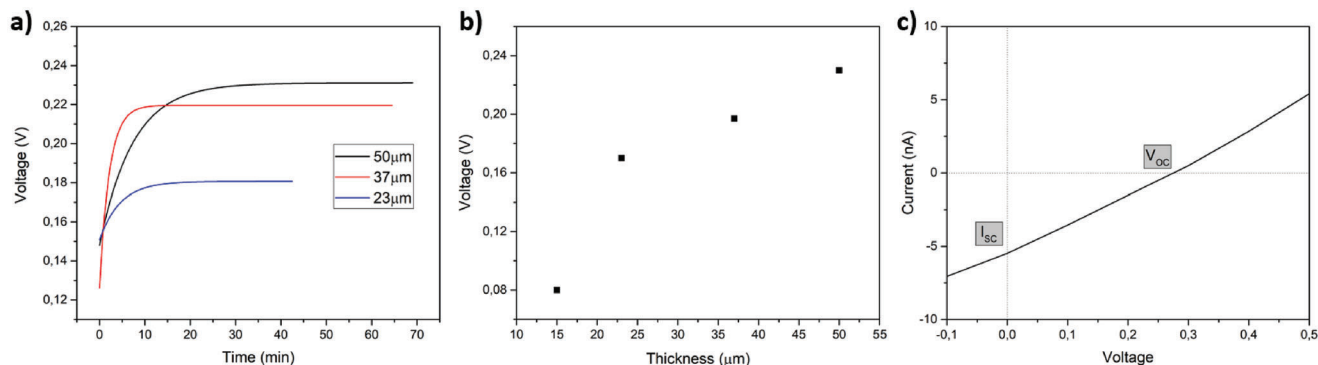


**Figure 5.** Electrical and electrochemical results varying the membrane thickness. a) OCP variation in time (original data in Figure S5, Supporting Information). b) OCP values obtained at different thicknesses. c) IV curve for the most performant membrane (50  $\mu\text{m}$ ).

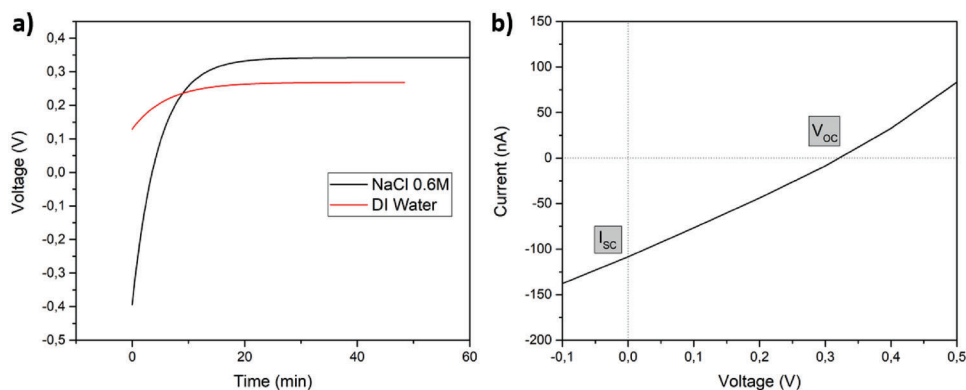


**Figure 6.** a) OCPs comparison between two GO membranes in different solutions. b) I–V of a GO membrane immersed in a NaCl solution.

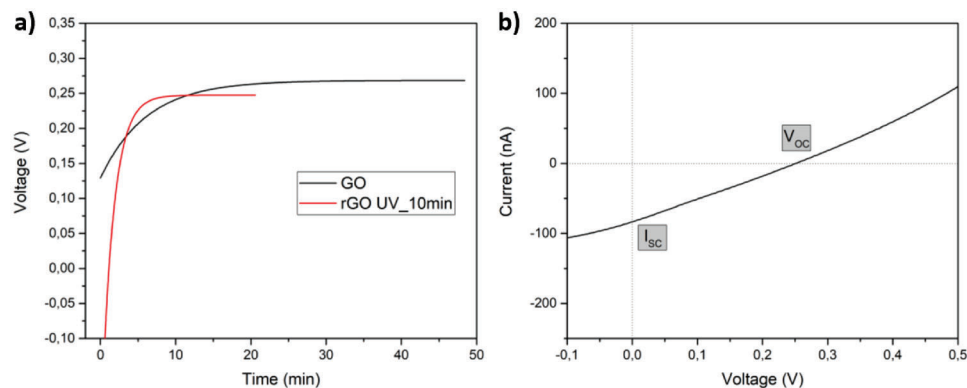


**Figure 7.** (a) OCPs comparison between two GO membranes before and after UV reduction. b)  $I$ - $V$  of a rGO membrane.

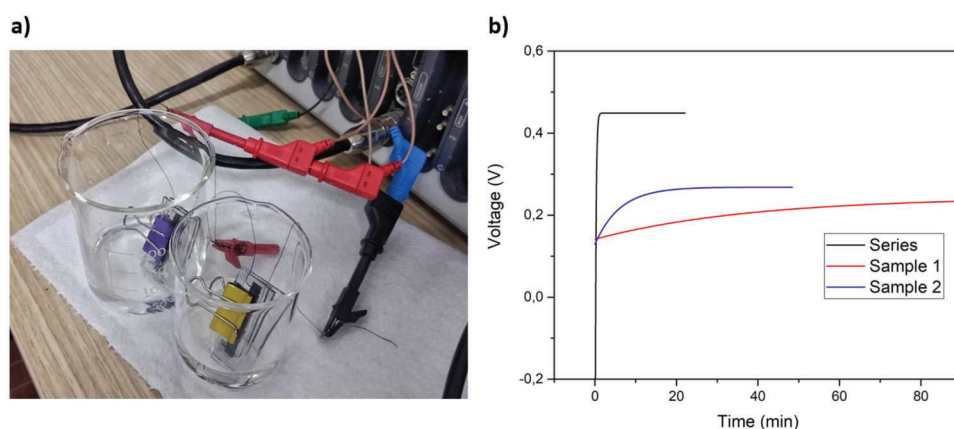


**Figure 8.** a) Digital photograph of the devices connected in series. b) OCPs evaluation of the devices connected in series compared to the results obtained on the single devices.

thickness (Figure 6b). The maximum output power reached in this configuration is  $20.8 \mu\text{W m}^{-2}$ .

Despite these good results, this experimental condition presents a problem of stability. Indeed, the NaCl solution seems to compromise the functionality of the GO membrane after almost two hours, limiting the possible application for long-term energy generation.

With the aim of maximizing the current while maintaining a good voltage value and ensuring high membrane stability, it was decided to verify the effect of the GO reduction. The reduction process of GO to rGO typically consists in a removal of some functional groups. Usually, this process occurs chemically in solution or thermally. Here instead we have decided to use a UV induced process that allows to partially reduce the membrane after it has already been manufactured, preserving its structural integrity. The membrane was exposed to UV light ( $6.37 \text{ W cm}^{-2}$ ) for 10 min (Figure S4, Supporting Information, shows the XPS spectra of the obtained material). Traditional chemical reductions act on GO flakes in solution with then greater difficulty in the formation of the stacked membrane. As it is possible to see in **Figure 7**, the reduction process does not affect the OCP while strongly enhancing the current, confirming that the water-carbon

surface interaction is the main responsible of the electricity generation.

Finally, considering a practical application of GO membranes for the generation of energy induced by water flow, two devices were connected in series to increase the working voltage. The results shown in **Figure 8** confirm that the series of the two devices generate an induced voltage that is almost equal to the sum of the OCPs of the two single devices.

### 3. Conclusions

In conclusion, the exploitation of GO membranes for electricity generation from water flow has been first reported. Previous literature underlines that hydrophilicity, surface functionalization, and controlled porosity are key requirements for carbon materials used for such application.

Since GO exhibits all these properties, it results in a promising candidate. A fluidic device was fabricated to host the GO membrane and the electrodes. The device was then inserted into a beaker and filled partially with water. A voltage generation between the bottom and the top side of the GO membrane was observed, induced by the capillarity and the water evaporation that

was essential for the correct operation of the experiment. OCP and IV measurements were conducted confirming the electricity generation induced by spontaneous water flow inside the 2D channels.

A correlation between membrane thickness and energy generation was found. The thicker the membrane, the higher the OCP. This can be due to the increased number of channels inside the membrane in which the water can pass. A saturation point was found at 50  $\mu\text{m}$ , above which the membrane presented structural defects.

Sea water was also investigated as a possible application scenario with improved current generation. However, the interaction with the ions reduced the capability of the membrane to produce a constant electrical current over time.

UV-reduction treatment was applied to the membrane to verify how the modification of the GO surface properties affects the electricity generation, resulting in a strong enhancement in the generated current.

Finally, a series connection check was made to further prove the validity of the experiments made. Taking two samples with same dimensions and very similar OCP, the induced voltage registered from their series was almost the sum of the two, confirming the hypothesis.

## 4. Experimental Section

Graphene oxide gel (2.5% wt.) was purchased from Graphenea. The gel was cast by Doctor Blade technique at different blade-to-substrate thicknesses from 0.5 mm to 3 mm and dried at room temperature; corresponding to final membrane thicknesses ranging from 15 to 50  $\mu\text{m}$ . Once dry, they were mechanically detached from the support.

X-Ray Diffraction (XRD) spectroscopy (X'Pert pro, Panalytical) was employed to measure the interlayer distance between GO sheets in the stacked membrane. Exploiting the well-known Bragg's law, the instrument was set to work with a Bragg–Brentano configuration, exploiting a Cu–K $\alpha$  source with  $\lambda = 1.541874 \text{ \AA}$ .

Electron microscopy characterization was carried out with a Field-Emission Scanning Electron Microscope (FESEM Supra 40, manufactured by Zeiss).

Fourier Transform Infrared (FTIR) spectroscopy (Nicolet 5700 FTIR) was performed directly on GO membranes in an attenuated total reflection (ATR) configuration.

Z-potential was measured by Zetasizer Nano ZS90 (Malvern) on solutions of GO obtained by a dilution of the gel in order to achieve a concentration of 10 mg L $^{-1}$ .

The surface chemistry of the membranes was investigated by X-Ray Photoelectron Spectroscopy (XPS), with a PHI 5000 VersaProbe (manufactured by Physical Electronics) equipped with Al K $\alpha$  radiation (1486.6 eV) as X-ray source. Wide-energy and high-resolution (HR) XPS spectra were processed using CasaXPS software (version 2.3.18). HR C1s core level spectra deconvolution into mixed Gaussian–Lorentzian individual components was obtained after binding energy (BE) calibration according to C1s position for graphitic C–C bonds (284.5 eV) and Shirley background subtraction.

The experimental setup for the electricity generation was prepared using two glass slides with the GO membrane sandwiched in the middle (see Figure S1 in the Supporting Information). The glass slide on the top had two holes for the inlet and outlet of water. Polydimethylsiloxane (PDMS, Kit 184 Dow Corning) was used as a gasket to avoid water path formation outside the GO membrane. Carbon nanotube (CNT) yarns (130  $\mu\text{m}$  diameter, Dexmat) were used as electrical contact with the GO membrane.

Electrical Measurements were Performed Using a Metrohm Autolab Pgstat128 Potentiostat/galvanostat for open circuit potential (OCP) mea-

surements and a Keithley 2440 source measure unit for current–voltage (I–V) characterizations. A polynomial fit was applied to interpolate the experimental data of the OCP curves in the paper, but an example of raw data is reported in Figure S2 in the Supporting Information.

## Supporting Information

Supporting Information is available from the Wiley Online Library or from the author.

## Conflict of Interest

The authors declare no conflict of interest.

## Data Availability Statement

The data that support the findings of this study are available from the corresponding author upon reasonable request.

## Keywords

blue energy, energy harvesting, graphene oxide, graphene oxide membranes, water

Received: February 7, 2023

Revised: April 11, 2023

Published online:

- [1] K. W. E. S, IEA **2020**, IEA, Paris <https://www.iea.org/reports/key-world-energy-statistics-2020>.
- [2] G. Liu, T. Chen, J. Xu, K. Wang, *J. Mater. Chem. A* **2018**, *6*, 18357.
- [3] B. E. Logan, M. Elimelech, *Nature* **2012**, *488*, 313.
- [4] Z. Jia, B. Wang, S. Song, Y. Fan, *Renewable Sustainable Energy Rev.* **2014**, *31*, 91.
- [5] K. Nijmeijer, S. Metz, in *Sustainability Science and Engineering*, Elsevier, New York **2010**, Vol. 2, 95.
- [6] a) A. Achilli, T. Y. Cath, A. E. Childress, *J. Membr. Sci.* **2009**, *343*, 42; b) Y. Mei, C. Y. Tang, *Desalination* **2018**, *425*, 156; c) D. Brogioli, *Phys. Rev. Lett.* **2009**, *103*, 058501. d) R. A. Tufa, S. Pawlowski, J. Veerman, K. Bouzek, E. Fontananova, G. di Profio, S. Velizarov, J. Goulão Crespo, K. Nijmeijer, E. Curcio, *Appl. Energy* **2018**, *225*, 290.
- [7] X. Qi, T. Miao, C. Chi, G. Zhang, C. Zhang, Y. Du, M. An, W. G. Ma, X. Zhang, *Nano Energy* **2020**, *77*, 10509.
- [8] R. K. Arun, P. Singh, G. Biswas, N. Chanda, S. Chakraborty, *Lab Chip* **2016**, *16*, 3589.
- [9] G. Zhang, Z. Duan, X. Qi, Y. Xu, L. Li, W. Ma, H. Zhang, C. Liu, W. Yao, *Carbon* **2019**, *148*, 1.
- [10] S. He, Y. Zhang, L. Qiu, L. Zhang, Y. Xie, J. Pan, P. Chen, B. Wang, X. Xu, Y. Hu, C. T. Dinh, P. De Luna, M. N. Banis, Z. Wang, T. K. Sham, X. Gong, B. Zhang, H. Peng, E. H. Sargent, *Adv. Mater.* **2018**, *30*, 1707635.
- [11] G. Xue, Y. Xu, T. Ding, J. Li, J. Yin, W. Fei, Y. Cao, J. Yu, L. Yuan, L. Gong, J. Chen, S. Deng, J. Zhou, W. Guo, *Nat. Nanotechnol.* **2017**, *12*, 317.
- [12] W. Olthuis, B. Schippers, J. Eijkel, A. Van Den Berg, *Sens. Actuators, B* **2005**, *111*, 385.
- [13] G. Z. Albert Tianxiang Liu, M. Strano, in *Robotic Systems and Autonomous Platforms*, Woodhead Publishing in Materials, Cambridge **2019**, p. 389.



- [14] P. Král, M. Shapiro, *Phys. Rev. Lett.* **2001**, *86*, 131.
- [15] T. Ding, K. Liu, J. Li, G. Xue, Q. Chen, L. Huang, B. Hu, J. Zhou, *Adv. Funct. Mater.* **2017**, *27*, 1700551.
- [16] a) A. Lamberti, *Mater. Sci. Semicond. Process.* **2018**, *73*, 106; b) L. Baudino, A. Pedico, S. Bianco, M. Periolatto, C. F. Pirri, A. Lamberti, *Membranes* **2022**, *12*, 233; c) N. Garino, A. Lamberti, S. Stassi, M. Castellino, M. Fontana, I. Roppolo, A. Sacco, C. F. Pirri, A. Chiappone, *Electrochim. Acta* **2019**, *306*, 106.
- [17] A. Pedico, M. Fontana, S. Bianco, S. Kara, M. Periolatto, S. Carminati, C. F. Pirri, E. Tresso, A. Lamberti, *Nanomaterials* **2020**, *10*, 2242.
- [18] P. Sun, H. Deng, F. Zheng, K. Wang, M. Zhong, Y. Zhang, F. Kang, H. Zhu, *2D Mater.* **2014**, *1*, 034004.
- [19] D. Chen, H. Feng, J. Li, *Chem. Rev.* **2012**, *112*, 6027.
- [20] E. Yang, H. E. Karahan, K. Goh, C. Y. Chuah, R. Wang, T. H. Bae, *Carbon* **2019**, *155*, 129.
- [21] R. K. Joshi, P. Carbone, F. C. Wang, V. G. Kravets, Y. Su, I. V. Grigorieva, H. A. Wu, A. K. Geim, R. R. Nair, *Science* **2014**, *343*, 752.
- [22] Y. Mao, M. Zhang, L. Cheng, J. Yuan, G. Liu, L. Huang, M. Barboiu, W. Jin, *J. Membr. Sci.* **2020**, 595.